A Rule-Based Advanced Static Var Compensator Control Scheme for Transient Stability Improvement

S. Abazari*, M. Ehsan[1], M.R. Zolghadri[1] and J. Mahdavi[1]

The paper presents the application of a rule- based control scheme for an Advanced Static Var Compensator (ASVC) to improve power system transient stability. The proposed method uses a current reference, based on the Transient Energy Function (TEF) approach. The proposed scheme provides, also, a continuous control of the reactive power flow. The performance of the proposed approach is compared with that of a system using a conventional control method and of a system without ASVC. A single-machine system and an IEEE three machine system are used to verify the performance of the proposed method.

INTRODUCTION

Transient stability is the ability of a power system to maintain synchronism when subjected to a serve disturbance. The resulting response of the system involves large excursions of generator rotor angle that are determined by the nonlinear power-angle relationship. System stability depends on both the initial operating condition of the system and the severity of the disturbance. Normally, transient stability for a large disturbance is studied for periods of up to several seconds [1].

The rapid development of power electronic devices in the last two decades has made it possible to design power electronic equipment of a high rating for high voltage systems.

Due to the fast control ability of these high rating static switches, fast transient response can be achieved in a system. An ASVC is a fully controlled switch based converter, which is an upgrade version of SVC, a thyristor based converter. Like an SVC, an ASVC provides a controllable parallel compensation. The reactive power generation or absorption by an ASVC is the same as that of an SVC. An ASVC has the following advantages over a conventional SVC:

1. An ASVC does not contain any energy storage components for providing reactive power. This has

---
*. *Corresponding Author, Department of Electrical Engineering, Shahrekord University, Shahrekord, I.R. Iran.*
1. *Department of Electrical Engineering, Sharif University of Technology, P.O. Box 11365-9363, Tehran, I.R. Iran.*

a great influence on minimizing the size and cost of an ASVC compared to a SVC of the same rating [2];

2. An ASVC generates harmonics with lower amplitude than those of a conventional SVC. Furthermore, the ASVC harmonics are at higher frequencies and can be filtered more easily [3];

3. An ASVC can control unbalanced loads more effectively [3];

4. Voltage regulation and transient stability enhancement by an ASVC are faster than a conventional SVC [4].

FACTS devices have been reported to significantly improve the transient and dynamic stability of power systems [5-8].

The ability of an ASVC to maintain full capacitive output current at a low system voltage also makes it more effective than SVC in improving transient stability [9]. The objective of this paper is to investigate the influence of ASVC on improving the transient stability of the power system using a rule based control scheme. ASVC is modeled as a sinusoidal current source, I_{ASVC}, whose reference value is determined by the proposed method. It is supposed that the ASVC inverter is controlled, such that it can follow the reference. The current reference is calculated using a Transient Energy Function (TEF) in a rule-based control scheme. Additional constraints, such as ASVCs maximum and minimum reactive power, due to device limits and bus voltage variations, are considered [9]. In [10], offline Lyaponov stability and

a linear programming theory are used to calculate the maximum or minimum of the current reference. Here, an online rule-based control scheme is used to calculate the ASVCs current reference. In this way, a continuous control of reactive power flow is achievable. Also, in [10], linear programming is used for current reference calculation, which requires a lot of calculation. In this paper, rule-based control is used, which has low complexity and can be implemented online.

ADVANCED STATIC VAR COMPENSATOR

Like SVC, an ASVC provides controllable parallel compensation of reactive power for a system. Basically, it consists of a GTO-based converter and a DC circuit (Figure 1). In the simplest form, the latter consists of a capacitor. ASVC ratings, limited by the switch ratings (voltage and current) and capacitor voltage, are:

-   Maximum capacitive current,

-   Maximum inductive current,

-   Minimum operating voltage for the inverter,

-   Maximum operating voltage (inverter rating),

which are shown in the U-I plane (Figure 2).

Control of reactive power is achieved through the switching scheme of the ASVC. In this way, the system can be supplied by the constant reactive current, I_{ASVC}, independent of the terminal voltage, U_{ASVC}. Therefore, considering the rating of the ASVC and neglecting its current harmonics, in the control system, ASVC is modeled as a sinusoidal current source, as shown in Figure 3.

The amplitude and phase of the ASVC current are two controllable parameters of the ASVC. To work as a reactive power compensator, the phase of the current
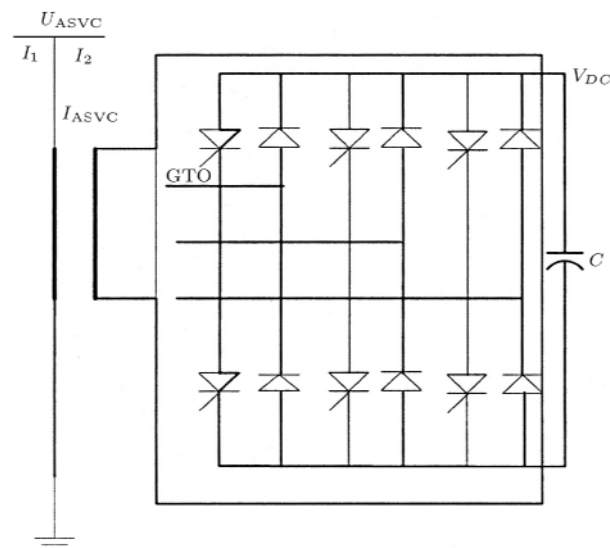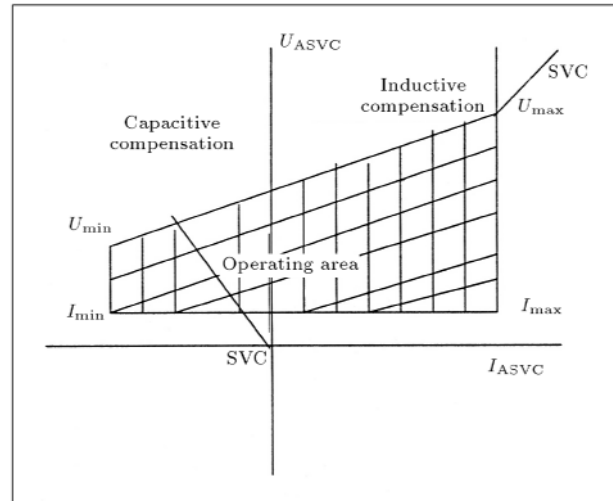

Figure 1. ASVC power circuit.

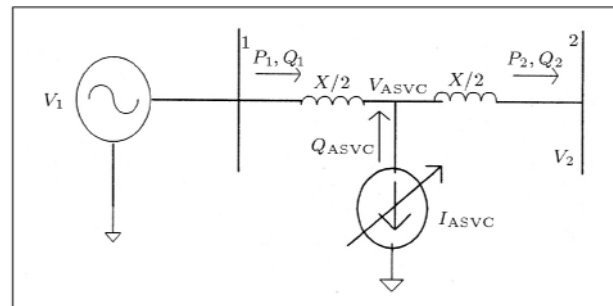**Figure 2.** ASVC and SVC operating characteristics.

Figure 3. Basic scheme of the ASVC.

is:

$$\mathrm{Arg}(I_{ASVC}) = \mathrm{Arg}(U_{ASVC}) \pm 90^\circ, \qquad (1)$$

in which Arg is the angle of a signal. 90° is selected to show that ASVC is a source of absorption or injection of reactive power.

In capacitive mode, vector I_{ASVC} leads and, in inductive mode, it lags voltage vector U_{ASVC} by 90°.

When an ASVC is connected to a transmission line, circumstances are basically similar to those of a SVC. As shown in Figure 2, the operating surface of ASVC is wider than that of SVC. In fact, ASVC can be used to compensate capacitive reactive power, as well as inductive reactive power, while, in SVC sets, it is limited by its inductive components (if any).

EFFECT OF ASVC ON TRANSIENT STABILITY

ASVC application can enhance the transient stability of the system by inserting or absorbing instantaneous current to or from the system. Its capability is verified for a single machine as follows [2].

Referring to Figure 3 for P_1 and Q_1, as well as P_2 and Q_2, the active/reactive power entering nodes 1

and 2, respectively, satisfy:

$$P_1 = P_2 = \frac{U_1 U_2}{X} \left[1 + \frac{I_{\text{ASVC}} X}{2 \sqrt{U_1^2 + U_2^2 + 2U_1 u_2 \cos \delta}} \right] \sin \delta, \quad (2)$$

$$Q_1 = \frac{U_1^2}{X} \quad \frac{U_1 U_2}{X} \cos \delta + \frac{I_{\text{ASVC}}}{2}, \quad (3)$$

$$Q_2 = \quad \frac{U_2^2}{X} + \frac{U_1 U_2}{X} \cos \delta \quad \frac{I_{\text{ASVC}}}{2}, \quad (4)$$

If $U_1 = U_2 = U$,

$$P_1 = P_2 = \frac{U^2}{X} \sin \delta + \frac{U I_{\text{ASVC}}}{2} \sin \frac{\delta}{2}, \quad (5)$$

where δ is the machine rotor angle. The second term in Equation 5 represents the increase or decrease in $P_{\max}$. It must be noted that I_{ASVC} in Equations 2 to 5 is a signed scalar, which is positive if the ASVC current is capacitive and negative if the ASVC current is inductive. I_{ASVC} varies between its maximum capacitive value ($I_{\max}$) and its minimum inductive negative value ($I_{\min}$). It is obviously seen that when ASVC injects its maximum current into the power system ($I_{\text{ASVC}} = I_{\max}$), P_1 is maximized and ASVC has its most significant contribution to transient stability improvement. On the other hand, when ASVC is in its inductive extreme, P_1 has its minimum value.

Transient Energy Function (TEF) can be used to calculate the margin of stability.

DESCRIPTION OF THE TEF APPROACH

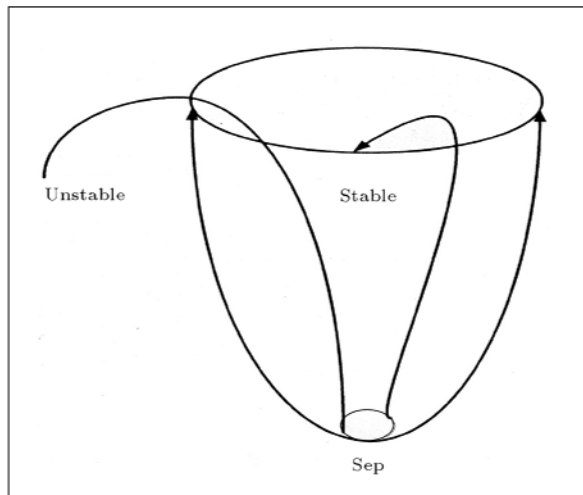The Transient Energy Function (TEF) approach can be described by considering a ball rolling on the inner surface of a bowl, as depicted in Figure 4 [9]. The area inside the bowl represents the region of stability and the area outside is the region of instability. The rim of the bowl is irregular in shape so that different points on the rim have different heights. Initially, the ball is resting at the bottom of the bowl. This state is referred to as the State Equilibrium Point (SEP). When the injected kinetic energy is high enough, it causes the ball to go over the rim. The surface inside the bowl represents the Potential Energy Boundary Surface (PEBS) [11-15]. Two quantities are required to determine whether the ball will enter the instability region: a) The injected initial energy and b) The height of the rim at the crossing point. The basis for the application of the TEF method for the analysis of power system stability is conceptually similar to that of a ball rolling in a bowl. If a fault occurs, the equilibrium point is disturbed and synchronous machines accelerate. The power system gains kinetic and potential energy during the fault and the system moves away from the SEP. After fault clearing, the kinetic energy, in the same manner as the ball rolling to the bowl, rolls up the potential energy surface. To avoid instability, the extra kinetic energy must be absorbed by the system to reach a new equilibrium point. This depends on the potential energy absorbing capability of the post disturbance system. By using an ASVC through the injection or absorption of reactive current, the transient energy margin increases.

Figure 5 shows the effect of ASVC to improve the transient stability using a bang bang control [2].

TEF FOR A MULTI MACHINE ASVC EQUIPPED SYSTEM

Swing equations for a multi-machine system can be explained as the following equations [1]:

$$\dot{\delta}_i = \omega_i \qquad i = 1, 2, \cdots, n, \quad (6)$$

$$M_i \dot{\omega}_i = P_i \quad D_i \quad \omega_i \quad P_{ei} \qquad i = 1, 2, \cdots, n, \quad (7)$$

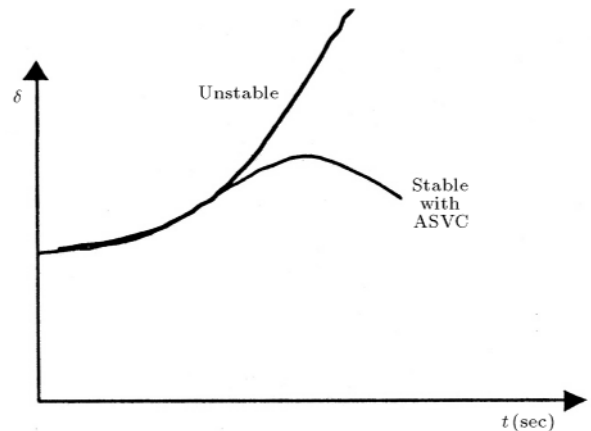**Figure 4.** A ball rolling on the inner surface of a bowl.

Figure 5. ASVC effect on transient stability.

where M_i is the ith machine, i.e., moment of inertia and D_i and P_{ei} are the damping factor and electrical power of the ith machine, respectively. In addition, D_i is assumed to be positive. P_i is the net transferred power, which is considered as a constant and has two terms:

$$P_i = P_{mi} \quad E_i^2 G_{ii}, \tag{8}$$

P_{mi} is the mechanical input power at the ith machine. Electric load in the ith node is considered as a constant impedance (G_{ii}). E_{ii} is the constant voltage behind the direct axis transient reactance of the ith machine. Node $n+1$ is the reference node, i.e., $E_{n+1} = 1, \delta_{n+1} = 0$. Electric power, P_{ei}, is:

$$P_{ei} = \sum_{j=1, j \neq i}^{n+1} E_i E_j (B_{ij} \sin \delta_{ij} + G_{ij} \cos \delta_{ij}), \tag{9}$$

G_{ij} and B_{ij} represent the transfer real and imaginary part of admittance between nodes i and j.

Pre-fault and post-fault systems equations differ in G's and B's, due to the variation in the network topology.

Adding k, ASVC sets introduce k additional nodes. In this case, the power equation will be modified to the form presented by the following equation:

$$P_{ei} = \sum_{j=1, j \neq i}^{n+1} E_i E_j (B_{ij} \sin \delta_{ij} + G_{ij} \cos \delta_{ij}$$
$$+ \sum_{j=1}^{n+\text{NAVC}} E_j B_{ij} \sin(\delta_{ij} \quad \phi_{j\text{ASVC}}), \tag{10}$$

where ϕ is angle of voltage ASVC. TEF has two potential and kinetic components. For the system with ASVC, TEF is presented by the following equation:

$$V(\delta, \omega) = V_{\text{PE}}(\delta, U_{\text{ASVC}}, \varphi_{\text{ASVC}}) + V_{\text{KE}}(\omega), \tag{11}$$

where V_{PE} is the potential energy and V_{KE} is the kinetic energy.

Since ASVC is blocked during the fault time; system equations during the fault are those presented in Equation 9. The TEF at post fault time can be written as:

$$V_{\text{PE}}(\delta, U_{\text{ASVC}}, \varphi_{\text{ASVC}}) = \sum_{i=1}^{n} P_{mi}(\delta_i \quad \delta_i^e)$$
$$\sum_{i=1}^{n} \sum_{j=n+1}^{n+n\text{ASVC}} |E_i| U_{j\text{ASVC}} B_{ij} [\cos(\delta_i \quad \varphi_{j\text{ASVC}})$$
$$\cos(\delta_i^e \quad \varphi_{j\text{ASVC}}^e)]$$
$$\sum_{i=1}^{n} \sum_{j=i+1}^{n} C_{ij} (\cos(\delta_{ij}) \quad \cos(\delta_{ij}^e)), \tag{12}$$

$$C_{ij} = |E_i||E_j|B_{ij}, \qquad V_{\text{KE}}(\omega) = \sum_{i=1}^{n} M_i \omega_i^2. \tag{13}$$

The notation, e, shows the equilibrium point. At the instability limit of the power system, $V(\delta, \omega)$ has its maximum permissible value. When the energy function exceeds this limit, the system becomes unstable. Therefore, the stability region of the power system is determined by:

$$V(\delta, \omega) \leq V_c, \tag{14}$$

where V_c is the energy function value at the Unstable Equilibrium Point (UEP).

The control strategy to improve the stability of the system must keep the energy function below the value given by Relation 14, in order to keep the state space trajectory within the stability region. The proposed control system must try to keep the energy function as close as possible to the minimum value (i.e. zero), in such a way that a trajectory of the system becomes closer to the stable point. In the other words, to improve system stability, the energy function must be minimized as much as possible. In order to reach a minimum energy function, the time derivation of $V(\delta, \omega)$ can be kept as negative as possible. On the other hand, this is the sufficient condition for Lyapunov stability. In order to match the overall Lyapunov criterion for stability, the derivation can be calculated as:

$$\frac{dV}{dt} = \frac{\partial V}{\partial \delta}.\dot{\delta} + \frac{\partial V}{\partial \omega}.\dot{\omega} + \frac{\partial V}{\partial U_{\text{ASVC}}}.\dot{U}_{\text{ASVC}} + \frac{\partial V}{\partial \varphi_{\text{ASVC}}}.\dot{\varphi}_{\text{ASVC}}, \tag{15}$$

$$\frac{\partial V}{\partial \omega_i} = \sum_{i=1}^{n} M_i \omega_i, \tag{16}$$

$$\frac{\partial V}{\partial \delta_i} = \sum_{j=i+1}^{n} P_{mi} + C_{ij} \sin \delta_{ij}$$
$$+ \sum_{i=1}^{n} \sum_{j=n+1}^{n+n\text{ASVC}} |E_i| B_{ij} \sin(\delta_i \quad \varphi_{j\text{ASVC}}), \tag{17}$$

$$\frac{\partial V}{\partial U_{j\text{ASVC}}} = \sum_{i=1}^{n} \sum_{j=n+1}^{n+n\text{ASVC}} |E_i| B_{ij} [\cos(\delta_i \quad \varphi_{j\text{ASVC}})$$
$$\cos(\delta_i^e \quad \varphi_{j\text{ASVC}}^e)], \tag{18}$$

$$\frac{\partial V}{\partial \varphi_{j\text{ASVC}}} = \sum_{i=1}^{n} \sum_{j=n+1}^{n+n\text{ASVC}} |E_i| B_{ij} V_{\text{ASVC}} [\sin(\delta_i \quad \varphi_{j\text{ASVC}})$$
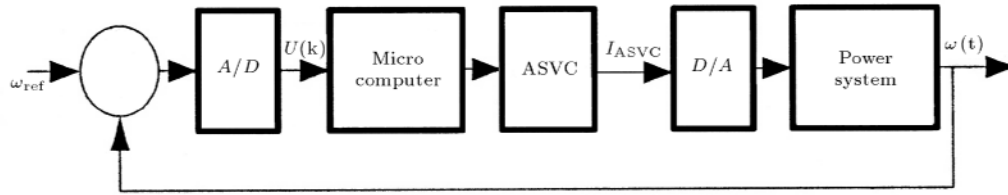$$\sin(\delta_i^e \quad \varphi_{j\text{ASVC}}^e)]. \tag{19}$$

Figure 6. Configuration of the proposed controller plane.

From Equations 7 and 12 to 18, the following is obtained:

$$\dot{V}(\delta,\omega) = \sum_{i=1}^{n} D_i \omega_i^2 \quad \sum_{i=1}^{n} \sum_{j=n+1}^{n+n\text{ASVC}} |E_i| B_{ij}$$

$$.[\cos(\delta_i \quad \varphi_{j\text{ASVC}}) \quad \cos(\delta_i^e \quad \varphi_{j\text{ASVC}}^e)]\dot{U}_{\text{ASVC}}$$

$$+\sum_{i=1}^{n} \sum_{j=n+1}^{n+n\text{ASVC}} |E_i| B_{ij} U_{j\text{ASVC}}[\sin(\delta_i \quad \varphi_{j\text{ASVC}})$$

$$\sin(\delta_i^e \quad \varphi_{j\text{ASVC}}^e)]\dot{\varphi}_{\text{ASVC}}. \qquad (20)$$

If $\dot{V}(\delta,\omega) < 0$, trajectories of the system will move towards the stability region. By linearizing Equation 16 about the operating point and neglecting machine damping, one will have:

$$\sum_{i=1}^{n} \sum_{j=n+1}^{n+n\text{ASVC}} |E_i| B_{ij} (U_{j\text{ASVC}} \quad U_{j\text{ASVCo}}) \Big[\cos(\delta_i \quad \varphi_{j\text{ASVCo}})$$

$$\cos(\delta_i^e \quad \varphi_{j\text{ASVC}}^e)\Big] + \sum_{i=1}^{n} \sum_{j=n+1}^{n+n\text{ASVC}} |E_i| B_{ij} U_{j\text{ASVCo}}$$

$$\sin(\delta_i \quad \varphi_{j\text{ASVCo}})(\varphi_{j\text{ASVC}} \quad \varphi_{j\text{ASVCo}}) > 0, \qquad (21)$$

where o represents the operating point index. Referring to the equations above, the absorption or rejection of the current can be controlled to agree with Inequality 21.

DETERMINATION OF CONTROL RULES

Configuration of the proposed rule-based controller is shown in Figure 6 for a single ASVC. It can be the closest ASVC to the fault in a multi ASVC system. The proposed controller is composed of a micro-computer with A/D and D/A converters. The supplementary stabilizing signal, ω, is calculated using the error signal of ω, which, inserted into the ASVC, controls the loop, as shown in Figure 7. The stabilizing signal, u, is given by:

$$u(t) = u(k) \qquad \text{for} \quad k\Delta T \leq t < (k+1)\Delta T. \qquad (22)$$

In discrete form, $u(k)$ is determined using machine states defined by $P(k)$, where $P(k)$ is:

$$P(k) = [\Delta\omega(k), \{\Delta\omega(k) \quad \Delta\omega(k \quad 1)/\Delta T]. \qquad (23)$$

The deviation of machine speed, $\Delta\omega$ (rad/sec), is measured at every sampling time and the acceleration of the machine is calculated by using the second term at the right hand side of Equation 23. The selection of the machine is according to Lyapunov's inequality, as stated in Inequality 21. In the phase plane, the upper half phase plane represents the positive acceleration; on the contrary, the lower half plane represents negative acceleration, i.e. deceleration. In addition, the points in the right-half plane represent the speeds faster than synchronous speed while the points in the left-half plane represent the speeds slower than synchronous speed. The origin, o, is the desired equilibrium point and all the control efforts should be directed to shift machine state, $P(k)$, towards the origin, o, as soon as possible. The phase plane is divided into six sectors, as shown in Figure 7. The amplitude of the current reference is chosen from the normalized value of the state vector, as a percent of the maximum or minimum of
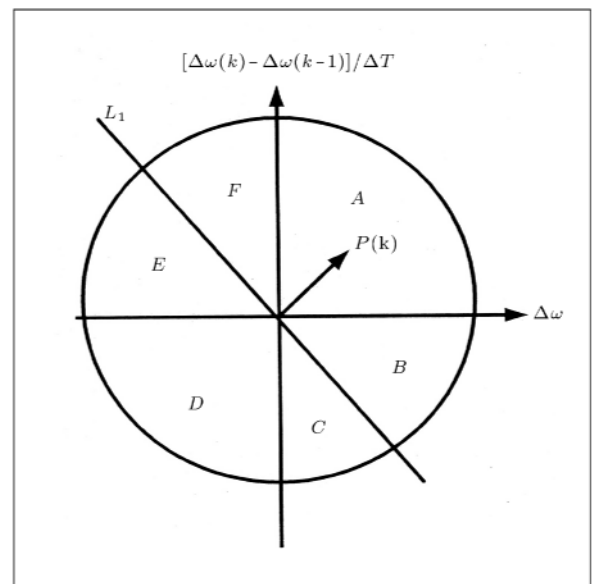

Figure 7. Six sectors in phase.

the current reference calculated from the optimization problem.

In sector A, the machine speed is almost equal to the synchronous speed but has a large acceleration. Then, a strong decelerating control of the controlled machine is required. Therefore, the control signal should be positive with a large value. In this case, the maximum value of the positive optimized current is used as the maximum value of the reference current.

In sector B, speed deviation is large and the machine has a negative acceleration. Therefore, with a small negative acceleration command, the machine continues to go toward the origin. In this sector, a small positive current reference is used. In this case, the minimum value of the positive optimized current is used as the value of the reference current.

In sector C, acceleration is large and negative and the speed is near the synchronous speed. To avoid decelerating more, a positive command will be applied (a negative small current). Therefore, the minimum negative value of the optimized current will be used as the current reference.

Sectors D, E and F are complementary with sectors A, B and C, respectively. Therefore, the command is complementary to those in zones A, B and C.

The small and large values used for the rule-based controller output are the outputs of an optimization program which is processed previous to application of the rule-based controller. The theory of the method is presented in the following section.

Rotating L as the borderline of Zones B, C and E, F can change the performance of the rule-based method, but, in this study, it is considered as a 135-degree line.

CALCULATION OF CURRENT REFERENCE

The optimized current trajectory is calculated minimizing a cost function presented in Equation 24. Linear programming is used to minimize this cost function with equality and inequality constraints presented with Equations 25 to 36.

$$\min \sum_{i=1}^{n} |\delta_i \quad \delta_i^e| + |\omega_i \quad \omega_i^e|, \qquad (24)$$

where δ_i^e and ω_i^e are equilibrium rotor angle and angular velocity, respectively.

Equation 25 is the linearized form of Equation 3 and Equation 26 is the linearized version of Equation 21.

$$M_i\omega_i \quad P_i\Delta t \quad P_{ei}\Delta t = 0,$$

$$i = 1, 2, \cdots, n, \qquad (25)$$

where:

$$P_{ei} \triangleq P_{eio} + \sum_{j=1}^{n\text{ASVC}} |E_i||y_{dij}| \Big[(\cos(\theta_{ij} \quad \delta_{io} + \varphi_{j\text{ASVCo}})\Delta U_{j\text{ASVCo}}$$

$$\sin(\theta_{ij} \quad \delta_{io} + \varphi_{j\text{ASVCo}})U_{j\text{ASVCo}}\Delta \Phi_{j\text{ASVC}}, \quad (26)$$

θ_{ij} and $|y_{dij}|$ are the phase and amplitude of the elements of the post fault reduced admittance matrix.

The dimension of the admittance matrix is equal to the number of ASVCs (nASVC) plus the number of machines (n). The admittance matrix post fault equation is expressed as follows:

$$Y_{\text{reduce}} = \begin{bmatrix} Y & Y \\ GG & GD \\ Y & Y \\ DG & DD \end{bmatrix}, \qquad (27)$$

where:

$$\frac{Y}{GG} \triangleq \begin{bmatrix} y_{g11} & y_{g12} & \cdot y_{g1i} & \cdot y_{g1n} \\ y_{g21} & y_{g22} & \cdot y_{g2i} & \cdot y_{g2n} \\ \cdots & \cdots & \cdot & \cdots \\ y_{gi1} & y_{gi2} & \cdot y_{gii} & \cdot y_{gin} \\ \cdot & \cdots & \cdots & \cdots \\ y_{gn1} & y_{gn2} & \cdot y_{gni} & \cdot y_{gnn} \end{bmatrix}, \qquad (28)$$

$$\frac{Y}{GD} = \frac{Y^T}{DG} \triangleq$$

$$\begin{bmatrix} y_{dg11} & y_{dg12} & \cdots & \cdots & y_{dg1n} \\ y_{dg21} & y_{dg22} & \cdots & \cdots & y_{dg2n} \\ \cdots & \cdots & \cdots & & \\ y_{dgi1} & y_{dgi2} & \cdots & \cdots & y_{dgin} \\ \cdots & \cdots & \cdots & & \\ y_{dgn\text{ASVC}1} & y_{dgn\text{ASVC}2} & \cdots & & y_{dgn\text{ASVC}n} \end{bmatrix}, \qquad (29)$$

and:

$$\frac{Y}{DD} \triangleq$$

$$\begin{bmatrix} y_{d11}+y_1 & y_{d12} & \cdots & y_{d1n\text{ASVC}} \\ y_{d21} & y_{d22}+y_2 & \cdots & y_{d2n\text{ASVC}} \\ \cdots & \cdots & \cdots & \cdots \\ y_{dgn\text{ASVC}1} & y_{dn\text{ASVC}2} & \cdots & y_{dn\text{ASVC}n\text{ASVC}} \\ & & & +y_{n\text{ASVC}} \end{bmatrix}, \qquad (30)$$

where $y_1, y_2, \cdots, y_{n\text{ASVC}}$ can be expressed as:

$$y_j = \frac{JQ_{j\text{ASVC}}}{U_j^2}, \qquad j = 1, 2, \cdots, n\text{ASVC},$$

$$J^2 = \quad 1. \qquad (31)$$

In the above equation, $Q_{j\text{ASVC}}$ and V_j are the injected reactive power and bus voltage of the ASVC, respectively. Considering $I = YV$, one can write:

$$\begin{bmatrix} I \\ G \\ I \\ \text{ASVC} \end{bmatrix} = \begin{bmatrix} Y & Y \\ GG & GD \\ Y & Y \\ DG & DD \end{bmatrix} \begin{bmatrix} E \\ G \\ U \\ \text{ASVC} \end{bmatrix}, \quad (32)$$

where $I_{\text{ASVC}} = 0$.

Due to the fact that the injected or absorbed current is modeled by admittance, therefore:

$$\frac{I}{G} = \begin{pmatrix} Y & Y & Y & Y & ^1 & Y \\ GG & GD & DD & DD & & DG \end{pmatrix} \frac{E}{G}. \quad (33)$$

The electric power is then calculated from:

$$P_{ei} = \text{Re}(E_i I_{gi}^*), \quad (34)$$

where * means conjugate. Moreover, the bus voltage of the ASVC must satisfy the following condition:

$$U_{iL} \leq U_{i\text{ASVC}} \leq U_{iH}, \quad (35)$$

where U_{iL} and U_{iH} are the lowest and highest permissible voltages at bus i, respectively. The ASVC must also satisfy:

$$Q_{\text{ASVC min}} \leq Q_{\text{ASVC}} \leq Q_{\text{ASVC max}},$$

$$Q_{\text{ASVC}} = yU_{\text{ASVC}}^2. \quad (36)$$

Considering the objective function in Relation 24 and using linear programming, the amount of absorbed/injected current can be calculated at each time step of the simulation. Since the Lyaponov stability condition is taken into account during the linear programming, a trajectory of the system will move towards the stability region.

TYPICAL SIMULATION RESULTS

In the first case, a single machine and infinite bus is considered. The ASVC is installed in the middle of the line, as shown in Figure 8. The line and machine characteristics are shown in Tables 1 to 3. A three-phase fault is simulated at the machine bus. The critical clearance time without ASVC is 0.175 sec. For the system with an ASVC in the middle of the line and controlled using the proposed scheme, it is supposed

Table 1. Line characteristics ($S_{\text{base}} = 300$ MVA and $V_{\text{base}} = 400$ KV).

Start	End	Series Resistance	Series Reactance
1	3	0.0199	0.075
2	3	0.0199	0.075

Figure 8. Single machine system.

Table 2. Bus data for the load flow calculations ($S_{\text{base}} = 300$ MVA and $V_{\text{base}} = 400$ KV).

Bus	Bus Type	Voltage	P_G	Q_G	P_L	Q_L
1	Slack	1	-	-	-	-
2	P-V	1	0.4	-	-	-
3	P-V	1	0	-	-	-

Table 3. Machinery data ($S_{\text{base}} = 300$ MVA).

X_s	H	D
0.312	2.035	0

that the clearance time of the fault breaker is 0.18 sec. Simulated rotor angle and angular velocity are shown in Figures 9 and 10, respectively. From Figures 9 and 10, one can see that the proposed control scheme of the ASVC can increase the critical time and avoid system instability.

In the second case, an IEEE 9-bus system is used

Figure 9. The rotor angle: a) Without control, b) ASVC with conventional bang-bang strategy and c) ASVC with the proposed control strategy.

Figure 10. The angular velocity: a) Without control; b) ASVC with conventional bang-bang strategy and c) ASVC with the proposed control strategy.

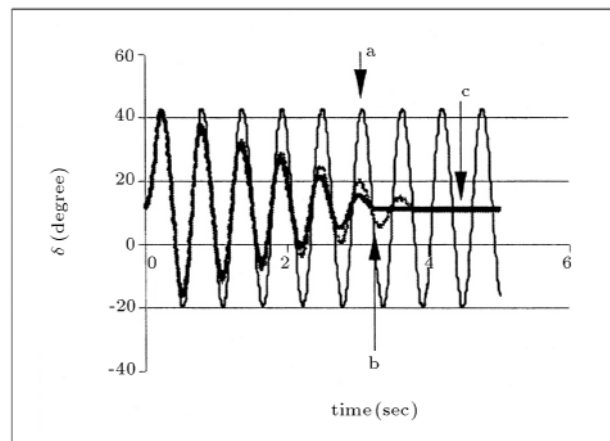**Table 4.** Characteristics of a three-machine system ($S_{\text{base}} = 100$ MVA).

Start Bus	End Bus	Series Resistance	Series Reactance	Half Admit.
2	7	0	0.0625	0
7	5	0.0320	0.1610	0.1530
5	4	0.0100	0.0850	0.088
4	6	0.0170	0.0920	0.0790
6	9	0.0390	0.1700	0.1790
8	9	0.0119	0.1008	0.1045
8	7	0.0085	0.0720	0.0745
3	9	0	0.0586	0
1	4	0	0.0576	0

(Figure 11). Machine 1 is the reference. The system characteristics are shown in Tables 4 to 6. The ASVC capacity is 200 MVAR. The optimal location of the ASVC is set on bus 4. In the simulation studies, a three-phase-to-ground fault at bus 7 is considered. While the critical clearance time is 0.227 sec., the fault

Figure 11. Three-machine system.

Table 6. Data of a three-machine system ($S_{\text{base}} = 100$ MVA).

No. Gen.	X_d	X_d'	X_q	H (sec)
1	0.146	0.0608	0.0969	23.64
2	0.8956	0.1198	0.8645	6.4
3	1.3125	0.1813	1.2576	3.01

clearing time is supposed to be 0.25 sec.

Three different situations are simulated to verify the performance of the proposed control scheme:

I.   Without any control,

II.   An ASVC with the conventional bang-bang control,

III. An ASVC with the proposed control strategy.

The behavior of machine 2 is shown in Figures 12 and 13 because this machine is the most affected. As can be seen in these figures, the system is stable with the proposed control strategy and unstable without any control action.

The simulation results show that out of the two

Table 5. Bus data for the load flow calculation ($S_{\text{base}} = 100$ MVA).

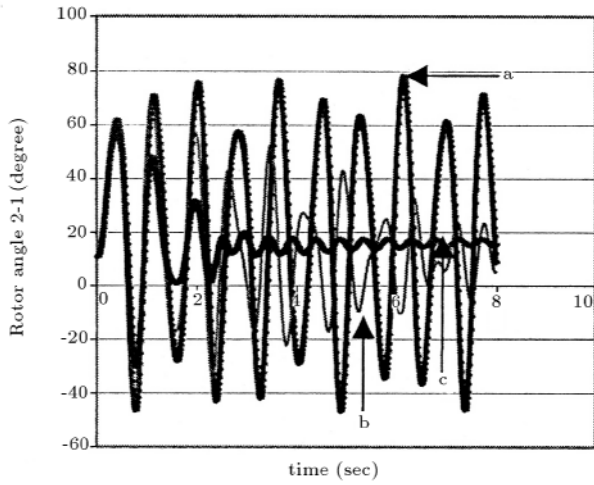| Bus	P_G (p.u.)	Q_G (p.u.)	P_L (p.u.)	Q_L (p.u.)	Voltage (p.u.)	Phase (Deg.)
1	0.71	0.27	0	0	1.04	0
2	1.63	0.06	0	0	1.02	9.3
3	0.85	-0.11	0	0	1.02	4.7
4	0	0.05	0	0	1.02	-2.2
5	0	0	1.25	0.50	0.99	-4
6	0	0	0.90	0.30	1.01	-3.7
7	0	0	0	0	1.02	3.7
8	0	0	1	0.35	1.01	0.7
9	0	0	0	0	1.03	2

Figure 12. The rotor angle of machine 2: a) Without control, b) ASVC with the conventional bang-bang strategy and c) ASVC with the proposed control strategy.
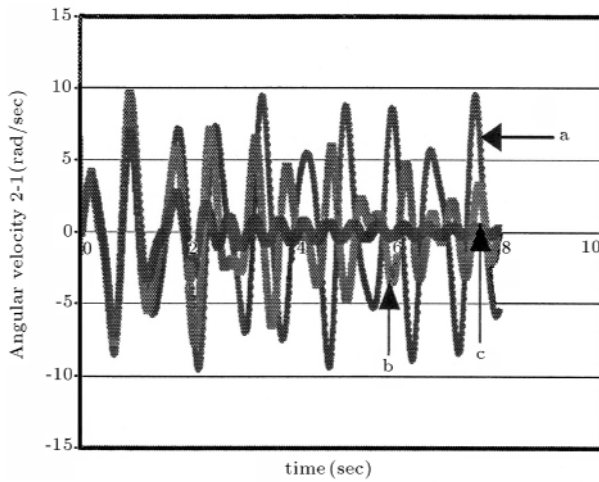

Figure 13. The angular velocity of machine 2: a) Without control, b) ASVC with the conventional bang-bang strategy and c) ASVC with the proposed control strategy.

cases, the proposed scheme damps the rotor angle oscillation faster. In addition, as can be seen in Figure 14, the new method results in a continuous reactive power flow control, which, in turn, provides a better system stability.

Comparing the phase plane trajectory of the machines shows, once more, the superiority of the proposed method against the classical bang bang control of ASVC (Figures 15 and 16).

CONCLUSIONS

In this paper, a new rule-based control approach for ASVC has been proposed. A performance of the proposed control technique is compared with a conventional bang-bang method in improving the transient
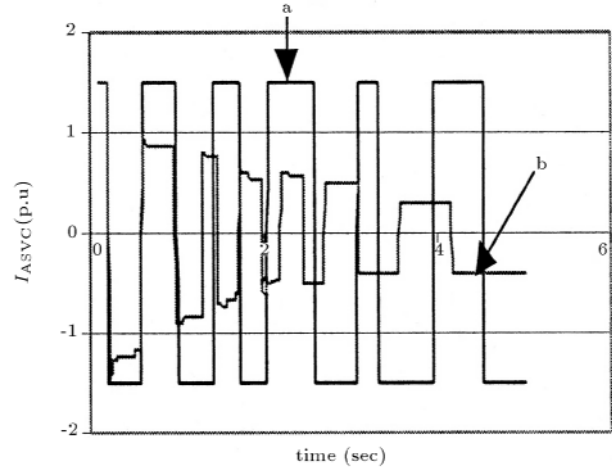

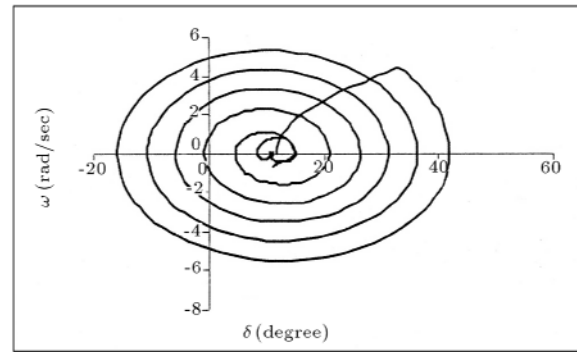**Figure 14.** Presentation of I_{ASVC}: a) Bang-bang control strategy and b) Proposed control strategy.

Figure 15. Phase plane δ, ω machine 2 with the bang-bang control strategy.
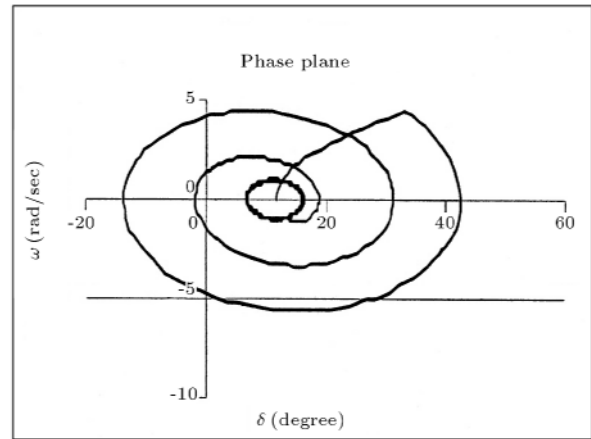

Figure 16. Phase plane δ, ω machine 3 with the proposed control.

stability of single-machine and multi-machine power systems. The simulation results confirm the ability of the proposed method to improve the transient stability of the system, as well as its superiority compared to the bang bang control of the ASVC.

Linear programming is used to calculate maxi-

mum and minimum inductive and capacitive currents. These values can be used to calculate ASVC current references in an online system using simple calculations.

REFERENCES

1. Kundur, P., *Power System Stability and Control*, Mc-Graw Hill (1993).

2. CIGRE Task Force 38.01.06, "Load flow control in high voltage power systems using FACTS controllers" (Jan. 1996).

3. *FACTS Overview*, CIGRE/IEEE Special Publication 95 TP 108 (April 1995).

4. Lerch, E. and Povh, P. "Performance of AC systems using FACTS equipment", *EPRI FACTS Conf.* (Dec. 1992).

5. Mihalic, R., Zunko, P., Papic, I. and Povh, D. "Improvement of transient stability by insertion of FACTS devices", in *Proc. Athens Power Tech. Joint International Power Conf.*, pp 521-525 (Sep. 1993).

6. Bortoni, G. "Impact of newly conceived flexible AC transmission system control strategies on the dynamic behavior of power system", *Stockholm Power Tech. Proceedings on Power Electronics*, pp 89-94 (June 1995).

7. Hingorani, N.G. "FACTS-flexible AC transmission systems", *2nd Annual Transmission & Wheeling Conference*, Denver, CO, USA (Nov. 1994).

8. Mihalic, R., Zunko, P. and Povh, D. "Improvement of transient stability using unified power flow controller", *IEEE Trans. on Power Delivery*, **11**(1), pp 485-492 (Jan. 1996).

9. Pai, M.A., *Energy Function Analysis for Power System Stability*, Kluwer Academic Publishing, Boston, USA (May 1989).

10. Abazari, S., Mahdavi, J. and Emadi, A. "Improvement transient stability by using advanced static var compensator", *Electric Power Components and Systems*, **31**(4), pp 321-334 (April 2003).

11. Pai, M.A., *Power System Stability Analysis by the Direct Method of Lyapunov*, North Holland Publishing Co., New York, USA (1981).

12. Glover, J. and Sarma, M., *Power System Analysis and Design*, PWS Publishers (1986).

13. Ribbens-Pavella, M. and Evans, F.J. "Direct methods for studying of the dynamics of large scale electric power systems- A survey", *Automatic*, **21**(1), pp 1-21 (1985).

14. Machowski, J. and Nelles, D. "Power system transient stability enhancement by optimal control of static VAR compensators", *Electrical Power and Energy Systems*, **14**(6), pp 411-421 (Dec. 1992).

15. Larsen, E.V., Miller, N.W., Nilsson, S.L. and Lindgren, S.R. "Benefits of GTO-based compensation systems for electric utility applications", *IEEE Trans. on Power Delivery*, **7**(4), pp 2056-2064 (Oct. 1992).